Papilloma Development Is Delayed in Osteopontin-Null Mice: Implicating an Antiapoptosis Role for Osteopontin

Yu-Hua Hsieh,[1] M. Margaret Juliana,[2] Patricia H. Hicks,[1] Gong Feng,[1] Craig Elmets,[3,4] Lucy Liaw,[5] and Pi-Ling Chang[1,4]

Departments of [1]Nutrition Sciences, [2]Genetics, and [3]Dermatology and [4]Comprehensive Cancer Center, University of Alabama at Birmingham, Birmingham, Alabama and [5]Center for Molecular Medicine, Maine Medical Center Research Institute, Scarborough, Maine

Abstract

Osteopontin is a secreted, adhesive glycoprotein, whose expression is markedly elevated in several types of cancer and premalignant lesions, implicating its association with carcinogenesis. To test the hypothesis that induced osteopontin is involved in tumor promotion *in vivo*, osteopontin-null and wild-type (WT) mice were subjected to a two-stage skin chemical carcinogenesis protocol. Mice were initiated with 7,12-dimethylbenz(a)anthracene (DMBA) applied on to the dorsal skin followed by twice weekly application of 12-*O*-tetradecanoylphorbol-13-acetate (TPA) for 27 weeks. Osteopontin-null mice showed a marked decrease both in tumor/papilloma incidence and multiplicity compared with WT mice. Osteopontin is minimally expressed in normal epidermis, but on treatment with TPA its expression is highly induced. To determine the possible mechanism(s) by which osteopontin regulates tumor development, we examined cell proliferation and cell survival. Epidermis from osteopontin-null and WT mice treated with TPA thrice or with DMBA followed by TPA for 11 weeks showed a similar increase in epidermal hyperplasia, suggesting that osteopontin does not mediate TPA-induced cell proliferation. Bromodeoxyuridine staining of papillomas and adjacent epidermis showed no difference in cell proliferation between groups. However, terminal deoxynucleotidyl transferase–mediated dUTP nick end labeling analyses indicated a greater number of apoptotic cells in DMBA-treated skin and papillomas from osteopontin-null versus WT mice. These studies are the first to show that induction of the matricellular protein osteopontin facilitates DMBA/TPA-induced cutaneous carcinogenesis most likely through prevention of apoptosis. (Cancer Res 2006; 66(14): 7119-27)

Introduction

The development of cancer is a multistage process, which has been operationally divided into three distinct stages: initiation, promotion, and progression. The initiation stage is defined by permanent genetic changes, which occur spontaneously or on exposure to carcinogen(s). Tumor promotion is defined as the stage in which selective initiated cells in a "conducive environment" acquire proliferative abilities that lead to the generation of benign tumors, such as papillomas. The tumor progression stage involves additional mutations and epigenetic changes, resulting in malignant tumor formation.

The mechanisms of tumor promotion are still not fully understood. Because an initiated cell may die or remain dormant for an extended period before acquiring proliferative abilities, the tumor promotion stage is considered the first rate-limiting step to tumor development. Although deregulation of cellular molecules, such as proto-oncogenes, and tumor suppressors plays a critical role in the process of tumorigenesis, recent studies have shown that the extent to which a specific proto-oncogene contributes to tumor development is highly dependent on the matrix microenvironment (1, 2). Thus, alterations in the microenvironment, such as increased expression of or changes in the composition of matrix molecules and/or cell surface receptors, may dictate the fate of an initiated cell. To further define the importance of matrix protein in tumor development, we studied the role of a tumor promoter-inducible protein, osteopontin, *in vivo*.

Osteopontin is a secreted, acidic, adhesive glycoprotein postulated to have calcium binding, chemotaxis, cell binding, and cell-signaling properties (3, 4). Depending on the tissue and/or the stimulant, osteopontin may be secreted as a minimal to highly phosphorylated protein (5, 6). One important characteristic of osteopontin is its ability to bind to surface receptors through the argininyl-glycyl-aspartic acid (RGD) cell-binding residues and other specific regions that mediate binding to integrin receptors and hyaluronic acid receptor CD44 (4, 7). The adhesion of osteopontin with these surface receptors *in vitro* has been shown to regulate the expression of genes encoding molecules, such as the inducible nitric oxide synthase, the α_1 integrin subunit, and the hepatocyte growth factor receptor (MET), to bind and/or activate pro-matrix metalloproteinase-3 (pro-MMP-3) and pro-MMP-9, and to activate phosphatidylinositol 3-kinase (PI3K)/protein kinase B pathway, leading to promotion of cell migration and cell survival (8–10).

Normally, osteopontin is predominantly expressed in bone and selective soft tissues, such as kidney, and in some body fluids. Interestingly, osteopontin-null or osteopontin-deficient mice (11, 12) show no developmental abnormalities or gross bone deformities unless intervention studies are done, suggesting protein redundancy for normal development and differentiation and that overexpression of osteopontin is more important in pathologic conditions, such as tumor development. Elevated expression of osteopontin has been reported in benign (13–15) and malignant tumors from organs, such as brain, breast, mouth, salivary glands, thyroid gland, lung, stomach, endometrium, ovary, kidney, colon, prostate, liver, and pancreas (10, 16, 17). Furthermore, elevated levels of osteopontin were detected in serum from breast, ovary, colon, prostate, pancreas, and lung cancer patients (10, 17). Collectively, these findings suggest that osteopontin may play an important role in tumorigenesis.

Requests for reprints: Pi-Ling Chang, Department of Nutrition Sciences, University of Alabama at Birmingham, 311 Susan Mott Webb Nutrition Sciences Building, 1675 University Boulevard, Birmingham, AL 35295-3360. Phone: 205-975-6624; Fax: 205-934-7049; E-mail: plchang@uab.edu.

doi:10.1158/0008-5472.CAN-06-1002

In previous studies, we used the *in vitro* "initiated" transformation sensitive (P+) epidermal JB6 cells and showed that induction of osteopontin is required for tumorigenic transformation of these cells (18). In this study, we used the two-stage (initiation-promotion) skin chemical carcinogenesis protocol to determine the role of osteopontin in tumor promotion *in vivo*. Mouse skin is ideal for studying the role of osteopontin in tumor development because (*a*) mouse epidermis expresses minimal levels of osteopontin (12, 19, 20), (*b*) osteopontin mRNA expression is increased by as early as 7 hours after 12-*O*-tetradecanoylphorbol-13-acetate (TPA) treatment (21), and (*c*) osteopontin is expressed in papillomas and squamous cell carcinomas (SCC) that arise in wild-type (WT) mice subjected to the two-stage skin chemical carcinogenesis protocol (19, 22).

Osteopontin-null (12) and WT mice were initiated with the carcinogen 7,12-dimethylbenz(a)anthracene (DMBA) followed by repetitive treatment with the tumor promoter TPA to determine whether the lack of osteopontin expression suppresses papilloma formation. We found that osteopontin-null mice exhibited a significant delay in tumor development. Osteopontin-null mice did not suppress TPA-induced epidermal hyperplasia nor was the proliferative capacity significantly different in the papillomas when compared with WT mice. Instead, we observed that osteopontin-null papillomas have more apoptotic cells than WT papillomas. Furthermore, DMBA-induced apoptosis study showed more apoptotic cells in the epidermis of osteopontin-null mice than in WT mice, implicating a prosurvival role for osteopontin. Thus, tumor promoter-induced osteopontin may prolong the survival of dormant initiated cells and thereby facilitate chemically induced tumor development.

Materials and Methods

Chemicals. TPA, bromodeoxyuridine (BrdUrd), acetone, and DMBA were purchased from Sigma (St. Louis, MO).

Osteopontin-null mice. Osteopontin-null mice, originally established in a hybrid of 129/SvJ × Black Swiss line (12), were backcrossed to 129S6/SvEv (Taconic, Germantown, NY), a subline of 129/SvJ, for four generations. Speed congenic analyses were used to select for mice with the highest percentage of 129S6/SvEv genotype. All heterozygous osteopontin-null mice consisting of at least 95% 129S6/SvEv markers were backcrossed for an additional five generations followed by expansion and generation of homozygous osteopontin-null mice. Genotyping was done by PCR as described previously (12).

Two-stage mouse skin chemical carcinogenesis protocol. All experimental procedures were done with institutional approval for animal use. Ten-week-old WT 129S6/SvEv mice (12 male and 12 female), purchased from Taconic, and homozygous osteopontin-null mice (12 male and 8 female), as described above, were subjected to the initiation-promotion protocol. Mice were shaved and treated with a chemical depilatory (Nair) for 1 minute, 4 days before initiation with 43.7 nmol DMBA in 200 μL acetone applied to the dorsal skin. Beginning 1 week later, 5 μg TPA in 200 μL acetone was applied twice weekly for 27 weeks. Negative control groups for both WT and osteopontin-null mice were treated with acetone the 1st week followed by acetone twice weekly (acetone/acetone) or DMBA followed by acetone (DMBA/acetone) or acetone followed by TPA (acetone/TPA). The number of tumors that measured >1 mm in diameter was counted, and body weight was recorded weekly. The length and width of each individual tumor were measured with calipers. The experiment was terminated at 33 weeks when WT mice reached 100% tumor incidence.

Dorsal skin and/or tumors were dissected from euthanized mice and fixed in 10% neutral-buffered formalin for <24 hours and paraffin embedded. Sections (5 μm) were stained with H&E for histopathologic analyses, which were done blinded.

Immunohistochemistry. Tumors and/or skin sectioned to 5 μm were deparaffinized and hydrated before blocking for endogenous hydrogen peroxidase. This was followed by blocking with biotin-free Fc receptor blocker (Innovex Biosciences, San Ramon, CA) and incubation overnight with 0.5 μg/mL or 1 hour with 5 μg/mL of purified anti-osteopontin polyclonal antibody (18) or preimmune purified rabbit IgG (negative control). Sections were rinsed and incubated with biotin-conjugated anti-rabbit antibody (InnoGenex, San Ramon, CA) followed by incubation with streptavidin conjugated to horseradish peroxidase (streptavidin-HRP; BioGenex, San Ramon, CA), and positive staining was visualized by incubation with 3,3′-diaminobenzidine (DAB) substrate (BioGenex). Slides were counterstained with hematoxylin and coverslipped.

Western blot analyses. Total protein was obtained by scraping the dorsal epidermis with a razor blade after treatment of the skin with 200 μL acetone or 5 μg TPA in 200 μL acetone. Scraped cells were lysed in a solution consisting of 50 mmol/L Tris (pH 7.4), 150 mol/L NaCl, 0.5% Triton X-100, 0.05% NaN_3, and protease inhibitors. Protein concentration was determined by the bicinchoninic acid method. Equal amounts of protein from each samples were run along with recombinant rat osteopontin (23), as positive control, and prestained protein markers (Amersham, Piscataway, NJ) in 10% SDS-polyacrylamide gels and transferred onto polyvinylidene fluoride membranes (Millipore, Billerica, MA) as described previously (18). Membranes were incubated with polyclonal anti-rat osteopontin or anti-glyceraldehyde-3-phosphate dehydrogenase (GAPDH). Primary antibody-binding sites were detected using secondary antibody coupled to HRP. Bands were visualized by chemiluminescence (Amersham).

ELISA. To quantify the amount of osteopontin induced by DMBA in the epidermis, total epidermis protein was analyzed by ELISA (Assay Designs, Ann Arbor, MI). In brief, microplate wells coated with an anti-osteopontin monoclonal antibody (mAb) were incubated with protein extract and washed. This was followed by incubation with a HRP-linked mAb to osteopontin. After incubation, the plates were washed and color substrate was added and incubated for 30 minutes. The reaction was stopped with hydrochloric acid solution. Absorbance values were detected at 450 nm. The final osteopontin concentration was normalized to 100 μg protein.

Epidermal hyperplasia. The dorsal skin of 10- to 11-week-old osteopontin-null and WT mice were shaved and Naired as described above. Five osteopontin-null mice and five WT mice were randomly selected and treated with 200 μL acetone or 5 μg TPA in 200 μL acetone once or every 3 days for a total of three treatments. These mice were sacrificed, and dorsal skin samples were paraffin embedded. Sections (5 μm) were stained with H&E, and epidermal thickness was evaluated as described in the figure legend.

BrdUrd incorporation and detection. At the conclusion of the skin chemical carcinogenesis study (33 weeks), mice were injected i.p. with 50 μg BrdUrd/g body weight 1 hour before sacrifice. Tumors with adjacent skin were collected, fixed, paraffin embedded, and sectioned to 5-μm sections. The BrdUrd *In situ* Detection kit (BD PharMingen, San Diego, CA) was used to identify proliferating cells. Briefly, slides were blocked for endogenous hydrogen peroxidase and antigen was retrieved by boiling in citric acid (pH 6.0) before incubation with anti-BrdUrd mAb conjugated to biotin. The slides were then incubated with streptavidin-HRP followed by DAB. Sections were counterstained with hematoxylin.

Terminal deoxynucleotidyl transferase–mediated dUTP nick end labeling assay. The analyses for apoptotic cells were done using tumors and skin of mice not injected with BrdUrd. Apoptotic cells were detected according to the procedure from Roche Diagnostics GmbH (Penzberg, Germany). Tissue sections were subjected to antigen retrieval using proteinase K followed by the addition of terminal deoxynucleotidyl transferase (TdT) enzyme and fluorescein-dUTP. Fluorescein-dUTP was detected by the addition of HRP-conjugated anti-fluorescein followed by the addition of DAB. As a positive control, slides were pretreated with DNase before treatment as described above.

DMBA effects on epidermis. Ten-week-old male WT and osteopontin-null mice were used. The dorsal skin was shaved and treated with a chemical depilatory as described above. The skin was treated with 20 μmol/L DMBA in 200 μL acetone and harvested at 100 hours after

treatment. Excised skin was fixed and paraffin embedded. Sections (5 μm) were used for TdT-mediated dUTP nick end labeling (TUNEL) analyses. The treatment of DMBA for 100 hours was determined from preliminary studies by analyzing epidermis for apoptotic cells at 24, 48, 72, and 100 hours of DMBA treatment. TUNEL-positive epidermal cells in DMBA-damaged skin were detected as described above.

Semiquantitative reverse transcription-PCR. Total RNA extracted from skin samples was transcribed to cDNA by reverse transcriptase using oligo(dT). Primers specific for mouse *spp1* were 5′-CTTTCACTCCAATC-GTCCCTA-3′ (forward) and 5′-GCTCTCTTTGGAATGCTCAAGT-3′ (reverse), which generated a 305-bp PCR product (24). To normalize expression of osteopontin, the forward primer 5′-CTCATGACCACAGTCCATGC-3′ and the reverse primer 5′-CACATTGGGGGTAGGAACAC-3′ were used to amplify a 200-bp segment of the housekeeping gene *GAPDH* (25).

Results

TPA induces osteopontin expression in the epidermis. Normally, the dorsal epidermis of male and nonpregnant female mice expresses minimal osteopontin mRNA (12, 20). We did immunohistochemical analyses on dorsal skin treated with or without TPA to confirm previous findings and to locate the site of osteopontin protein expression. Skin sections (5 μm) from osteopontin-null or WT mice treated with 200 μL acetone or 5 μg TPA in 200 μL acetone were incubated with a polyclonal antibody to rat osteopontin or rabbit IgG. Untreated WT or osteopontin-null dorsal epidermis (Fig. 1, *B* and *D*) did not stain with antibody to osteopontin. Likewise, no staining was observed in sections incubated with IgG as negative control (Fig. 1, *A, C, E*, and *G*). Compared with acetone-treated WT skin (Fig. 1*F*), TPA induced significant osteopontin protein expression in the epidermis (Fig. 1*H*), consistent with previous studies on osteopontin transcript level (21).

Lack of osteopontin expression suppresses benign tumor development. To determine whether the lack of osteopontin expression affects tumor development *in vivo*, osteopontin-null and WT 129 mice were treated topically with a single application of DMBA followed by treatment with TPA twice weekly for 27 weeks and sacrificed at 33rd week. Osteopontin-null mice exhibited delayed tumor development and reduced tumor multiplicity.

Interestingly, male osteopontin-null mice exhibited a delay in tumor/papilloma appearance compared with WT mice (Fig. 2*A, left*), whereas tumors began to appear at the same time in females mice from both groups (Fig. 2*A, right*). By 14.5 weeks of promotion, the WT male mice reached 50% tumor incidence (16 weeks for female WT mice), whereas osteopontin-null male mice did not reach 50% tumor incidence until 20 weeks (26 weeks for female osteopontin-null mice). By 27 weeks of promotion, the number of tumors per mouse was 2.1-fold higher for male WT mice than male osteopontin-null mice (Fig. 2*B, left*) and 3.3-fold higher for female WT mice than female osteopontin-null mice (Fig. 2*B, right*). The percentage of tumor incidence after 27 weeks of promotion was 91.7% for WT male mice compared with 75% for osteopontin-null male mice (Fig. 2*A, left*) and 85% for WT female mice compared with 50% for osteopontin-null female mice (Fig. 2*A, right*).

The negative control groups (acetone/acetone, DMBA/acetone, and acetone/TPA) in both WT and osteopontin-null mice did not develop papillomas (data not shown). The lower percentage incidence and tumor multiplicity in the osteopontin-null groups of both genders compared with WT mice were independent of body weight as there were no significant decreases in the body weight of osteopontin-null versus WT mice during the course of the experiment (Fig. 2*C*). These findings show that tumor promoter-induced osteopontin expression facilitates the development of chemically induced papilloma formation.

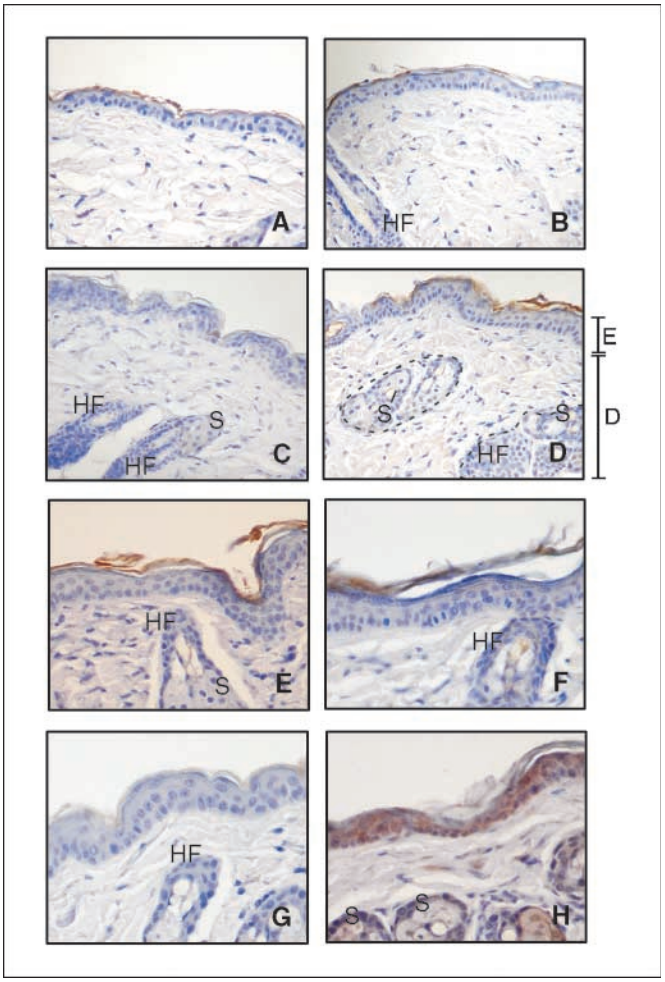

Figure 1. Expression of osteopontin in mouse skin of WT and osteopontin-null mice with and without TPA treatment. Sections (5 μm) of dorsal skin from untreated WT mice (*A* and *B*), untreated osteopontin-null mice (*C* and *D*), and WT mice treated with 200 μL acetone (*E* and *F*) or 5 μg TPA (*G* and *H*) were incubated with 0.5 μg/mL rabbit IgG (*A, C, E*, and *G*) or 0.5 μg/mL anti-osteopontin antibody (*B, D, F*, and *H*). *E,* epidermis; *D,* dermis; *HF,* hair follicle; *S,* sebaceous gland. Magnification, ×40 [not zoomed (*A-D*) and zoomed (*E-H*) before photographing with the Nikon 4500 digital camera; Nikon, Tokyo, Japan].

Histopathology of tumors from WT and osteopontin-null mice. Histopathologic examination of tumors and adjacent skin from female osteopontin-null mice at 33 weeks revealed that the tumors were all papillomas, whereas male osteopontin-null mice developed mostly papillomas with one keratoacanthoma and one SCC. The male WT mice developed mostly papillomas with three papillary hyperplasias, whereas the female WT mice developed mostly papillomas with two cases of keratoacanthomas.

WT and osteopontin-null mice show no difference in TPA-induced epidermal thickness or in proliferative capacity of their papillomas and adjacent epidermis. In an attempt to determine the mechanism by which the lack of osteopontin expression delays and suppresses tumor development, we hypothesized that osteopontin may prevent apoptosis and/or increase the proliferation of DMBA/TPA-treated cells and, therefore, facilitate the development of papillomas. To determine if osteopontin stimulates cell proliferation, we questioned whether osteopontin

is necessary for TPA-induced epidermal hyperplasia or cell proliferation (26). Treatment with 5 μg TPA once or thrice elicited a significant amount of osteopontin protein expression in WT mouse epidermis but, as expected, not in nontreated, acetone-treated, or osteopontin-null mice (Fig. 3*A*).

There was no significant difference in the epidermal thickness between osteopontin-null and WT mice treated with TPA thrice as shown by H&E staining (Fig. 3*B*) and as assessed by quantifying the number of epidermal cell layers (Fig. 3*C*). Likewise, no significant difference in the epidermal thickness was observed after initiation by DMBA followed by 11 weeks of TPA (DMBA/TPA) treatment (data not shown).

Analyses on the proliferative capacity of papillomas and adjacent epidermis were also done. Mice were injected with BrdUrd before sacrifice to label the proliferating cells in the papillomas and epidermis of osteopontin-null and WT mice. BrdUrd staining in the basal cell layer of papillomas and the adjacent epidermis was not different in both WT (Fig. 4*A, a-c*) and osteopontin-null mice (Fig. 4*B, a-c*; Table 1). These studies suggest that osteopontin does not mediate TPA-induced cutaneous hyperplasia nor affect the proliferation of papillomas and their adjacent epidermis.

Papillomas from osteopontin-null mice show more apoptotic cells, and osteopontin expression is found in WT papillomas. Analyses for apoptotic cells by TUNEL assay showed more prominent apoptotic cells in upper part of the spinous and granular layers of papillomas from osteopontin-null (Fig. 4*C, right, inset*) versus WT mice (Fig. 4*C, left, inset*). Additionally, the adjacent epidermis of osteopontin-null papillomas also appeared to contain apoptotic cells (Table 1). Because there were fewer papillomas in the osteopontin-null group and most of the osteopontin-null mice

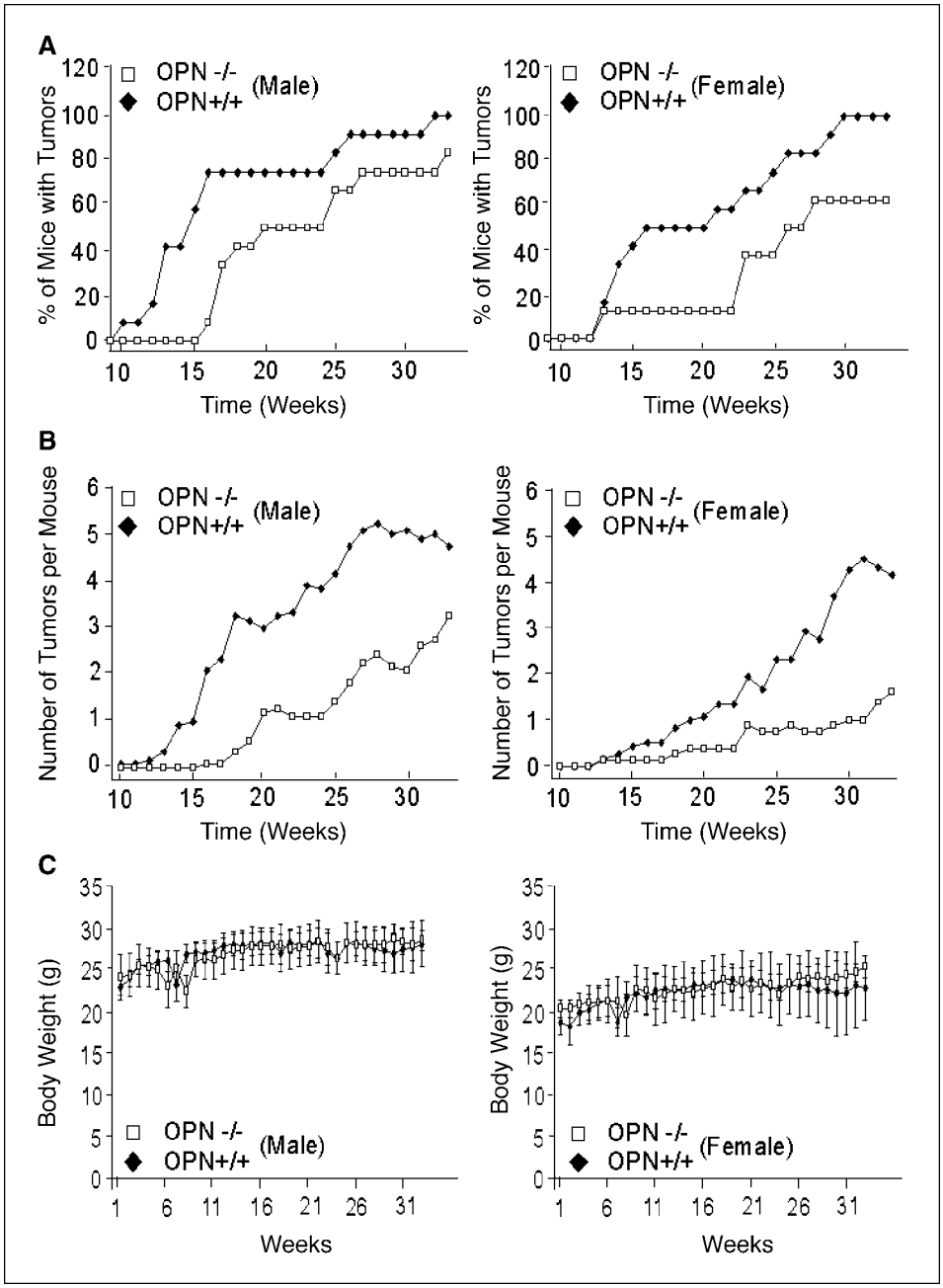

Figure 2. Tumor incidence, multiplicity, and body weight of osteopontin-null and WT mice in chemically induced skin carcinogenesis. WT ($OPN^{+/+}$; 12 males and 12 females) and osteopontin-null ($OPN^{-/-}$; 12 males and 8 females) mice were initiated with DMBA and, after 1 week, treated topically with TPA twice weekly for 27 weeks followed by 6 weeks of no treatment. Mice were sacrificed at 33 weeks. *A,* tumor incidence (% of mice with tumors). *B,* number of tumors per mouse (multiplicity). *C,* average body weight of mice. *A* to *C, left,* data for male $OPN^{+/+}$ and $OPN^{-/-}$ mice; *right,* data for female $OPN^{+/+}$ and $OPN^{-/-}$ mice.

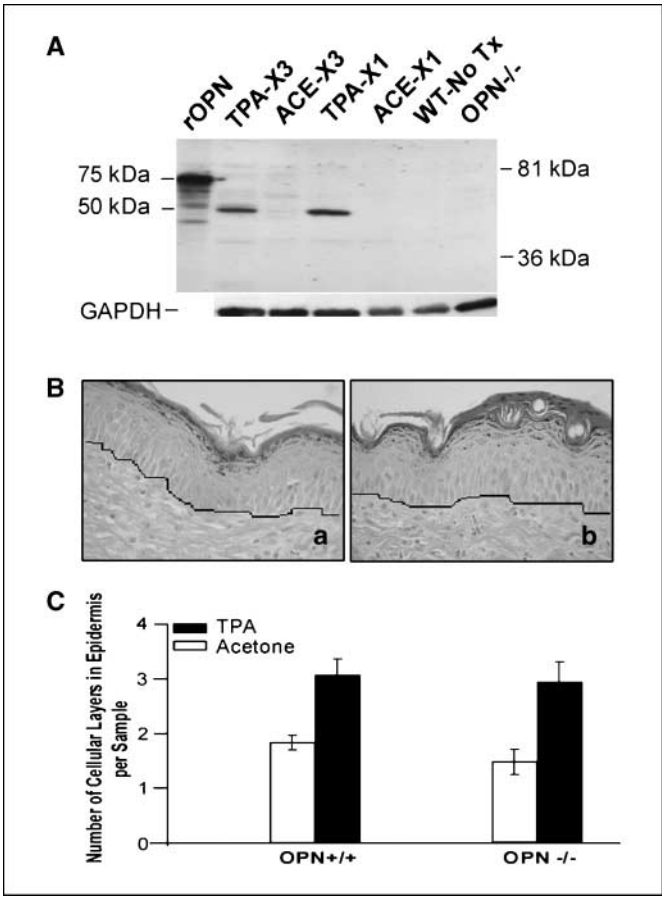

Figure 3. Osteopontin expression and epidermal hyperplasia in WT and osteopontin-null mice treated with TPA or acetone. *A,* osteopontin protein expression in WT epidermis treated with TPA or acetone. Dorsal skin of WT mice not treated (*WT-No Tx*), treated with 200 μL acetone once (*ACE-x1*) or thrice (*ACE-x3*; once every 3rd day), or treated with 5 μg TPA in 200 μL acetone once (*TPA-x1*) or thrice (*TPA-x3*; once every 3rd day). Skin was harvested 24 hours after the last treatment. Dorsal skin from untreated osteopontin-null mice ($OPN^{-/-}$) was also harvested. Protein (20 μg) from each sample and recombinant rat osteopontin (*rOPN*; 24 ng) were run in 10% SDS-PAGE followed by Western blot analyses. Note that, compared with mouse osteopontin, the recombinant rat osteopontin consists of an additional 59 amino acid residues. *B,* epidermal hyperplasia of WT and osteopontin-null skin. The dorsal skin of WT and osteopontin-null mice was treated thrice (once every 3 days) with TPA (5 μg/200 μL acetone) or acetone (200 μL). Skin was excised, fixed in formaldehyde, and paraffin embedded. Sections were stained with H&E. *a* and *b,* WT and osteopontin-null mouse skin treated with TPA, respectively. Skin from WT and osteopontin-null mice treated with acetone did not show epidermal hyperplasia (data not shown). *C,* histogram of the number of cell layers in the epidermis of WT and osteopontin-null mice treated with acetone or TPA thrice before sacrifice. Epidermal thickness was quantitated by counting number of layers of cells in the epidermis at intervals of 20 basal cells 10 times for TPA-treated and 7 times for acetone-treated skin. Two skin sections/slide per mouse were counted. *Columns,* average of five slides per group; *bars,* SD.

with tumors were first used for BrdUrd analyses, we were not able to assess all the adjacent epidermis surrounding the papillomas for apoptotic cells.

Because previous studies by Northern blot analyses have reported osteopontin expression in papillomas (19, 22), we analyzed immunohistochemically the localization of osteopontin protein. Osteopontin was observed in the upper part of the spinous and granular layers of WT papillomas and adjacent epidermis (data not shown) with minimal expression found in the tumor stroma (Fig. 4*D, a* and *b*).

Osteopontin expression suppressed DMBA-induced apoptosis of epidermal cells. To further determine if osteopontin promotes cell survival in injured epidermis, we treated mouse skin with 20 μmol/L DMBA to induce apoptosis. DMBA treatment led to increased expression of osteopontin by 24 hours, which persisted for 100 hours (Fig. 5*A*) as shown by semiquantitative reverse transcription-PCR (RT-PCR) from RNA samples of mouse skin and immunohistochemistry analyses (Fig. 5*B*). Further analyses of osteopontin protein by ELISA showed significant amounts of osteopontin in DMBA-treated WT epidermis (3.62 ± 1.8 ng/100 μg protein; $n = 3$) compared with acetone-treated (<0.9 ng/100 μg protein; $n = 3$) mice. TUNEL analyses of mouse skin at 100 hours after DMBA treatment showed markedly increased number of apoptotic cells in osteopontin-null basal cell layer than in WT (Fig. 5*C* and *D*). Thus, the induction of osteopontin could prevent apoptosis of both normal and carcinogen-initiated epidermal cells and, in so doing, can function as a facilitator of tumor development.

Discussion

Whether a matricellular protein, such as osteopontin, can influence the microenvironment and thereby facilitate tumorigenesis, we first investigated this possibility using the tumor-promotable JB6 cell line. We and others have shown that the tumor promoter TPA markedly enhances osteopontin synthesis and secretion and concomitantly stimulates tumorigenic transformation of these cells as assessed by colony formation in soft agar (5, 27, 28). TPA also increases the cell surface affinity or avidity of integrin (most likely $\alpha_v\beta_5$) in JB6 cells for osteopontin, thus implicating that tumorigenic transformation is facilitated by TPA-induced secretion of osteopontin localized around the cells when embedded in soft agar (29). Stable transfection of JB6 with antisense osteopontin resulted in suppressed expression and secretion of TPA-induced osteopontin and inhibited TPA-induced tumorigenic transformation, which was partially rescued on the addition of exogenous osteopontin (18). Furthermore, the addition of osteopontin to simulate overexpression also stimulates transformation of JB6 cells. Collectively, these studies support the requirement of TPA-induced expression of secreted osteopontin in facilitating tumorigenic transformation *in vitro*.

To address the role of osteopontin in carcinogenesis *in vivo*, two studies have been done. The first study shows that osteopontin-deficient (11) transgenic mice expressing both c-myc and v-Ha-ras, which have been shown to partially regulate osteopontin expression (30, 31), did not reduce mammary tumor development when compared with transgenic mice expressing osteopontin (32). The lack of reduction in mammary tumors could be due to the overexpression of two oncogenes, which stimulate compensatory proteins leading to robust mammary tumor development. The second *in vivo* study used an independently derived osteopontin-null mouse (12) to address the role of osteopontin in tumor progression, the second rate-limiting step in carcinogenesis. This one-stage skin carcinogenesis model requires a weekly application of the carcinogen *N*-methyl-*N*′-nitro-*N*-nitrosoguanidine for 40 weeks, which leads to multiple mutations and other epigenetic changes synonymous to the stage defined as tumor progression (33). Interestingly, this study found that the lack of osteopontin expression led to almost no papilloma formation but more SSCs and metastases when compared with WT mice. Whether the lack of papilloma formation in osteopontin-null mice was due to carcinogen-induced apoptosis and whether carcinogen treatment elicited osteopontin expression in WT mice were not addressed.

Despite these two studies, no report has directly addressed the role of osteopontin in the tumor promotion stage *in vivo*. The present study uses the two-stage mouse skin chemical carcinogenesis protocol (known as the prototype for tumor promotion study) to determine the function of osteopontin in benign tumor/papilloma development. We show that the lack of osteopontin expression in osteopontin-null mice markedly delayed the tumor incidence and reduced the number of tumors per mouse compared with WT mice. Additionally, relative to WT mice, an increase in the latency period of tumor development in osteopontin-null male but not in osteopontin-null female mice was observed. The reason for this gender difference in the latency period is not clear. However, it is also interesting to observe that, in both WT and osteopontin-null female mice, tumorigenesis seems to be delayed compared with males of corresponding group. Whether the gender difference is due to differences in sex hormones or chronic inflammation in males from persistent fighting remains to be investigated.

The delay in tumor development in both genders of osteopontin-null mice compared with WT mice occurred independently of body weight because no significant differences were observed between the body weights of osteopontin-null and WT mice during the time of tumor appearance. Consistent with previous reports on osteopontin transcript levels (12, 20), we observed that the dorsal epidermis of WT male and nonpregnant female mice expresses a minimal level of osteopontin protein, but on TPA treatment (once or thrice), the level of osteopontin protein is substantially increased (Fig. 3*A*). Thus, persistent expression of osteopontin in an initiation-tumor promotion skin carcinogenesis study suggests that alteration in the microenvironment by elevated osteopontin synthesis and secretion in the epidermis can facilitate the development of benign tumors.

To determine the mechanism by which elevated osteopontin expression might contribute to tumor development, we postulated that TPA-induced synthesis and secretion of osteopontin

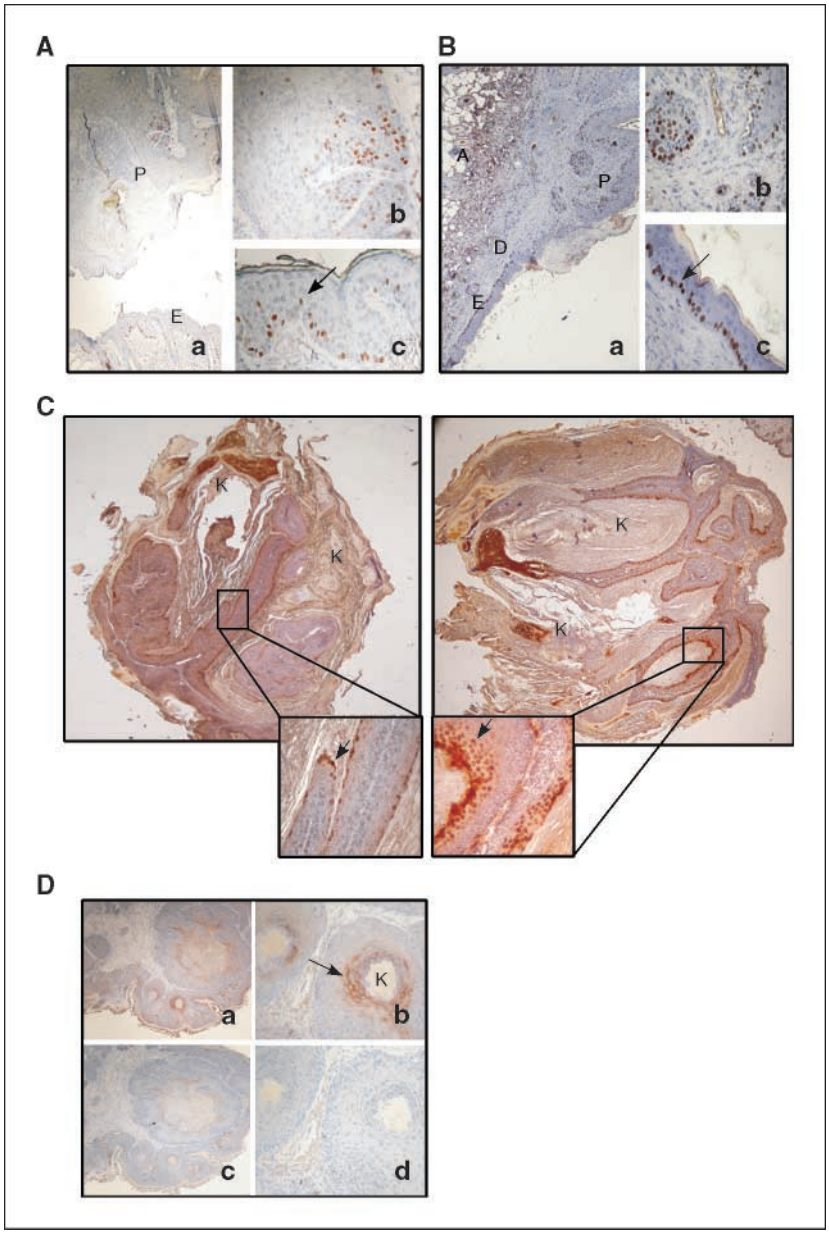

Figure 4. Osteopontin expression, proliferating and apoptotic cells in papillomas, and adjacent epidermis of osteopontin-null and WT mice. *A,* proliferating cells in papilloma (*P*) and adjacent epidermis (*E*) from WT mouse. *a,* papilloma from a WT mouse at 33 weeks probed with anti-BrdUrd mAb. Magnification, ×10. *b* and *c,* enlarged regions of papilloma and epidermis, respectively, from (*a*). Magnification, ×40. *B,* proliferating cells in a papilloma and adjacent epidermis of an osteopontin-null mouse. *a,* papilloma with adjacent epidermis from an osteopontin-null mouse at 33 weeks probed with anti-BrdUrd mAb. Magnification, ×10. *b* and *c,* enlarged regions of papilloma and epidermis, respectively, from (*a*). Magnification, ×40. *A,* adipose; *D,* dermis. *C,* apoptotic cells in papillomas from WT (*left*) and osteopontin-null (*right*) mice. Magnification, ×4. Sections of papillomas from WT and osteopontin-null mice not injected with BrdUrd were used for analyses of apoptotic cells using a TUNEL assay kit. *Insets,* enlarged papilloma regions from WT and osteopontin-null papillomas. Magnification, ×40. *K,* keratin. *D,* osteopontin expression in a papilloma from WT mouse. *a* and *b,* same section stained with polyclonal antibody specific to osteopontin. Magnifications, ×10 (*a*) and ×40 (*b*). *c* and *d,* consecutive sections of the same papilloma as in (*a*) and (*b*) probed with control purified rabbit IgG antibody. Magnifications, ×10 (*c*) and ×40 (*d*).

Table 1. BrdUrd and TUNEL-positive cells in papillomas and epidermis of WT and osteopontin-null mice

		Male		Female	
		$OPN^{+/+}$ (n = 7)	$OPN^{-/-}$ (n = 5)	$OPN^{+/+}$ (n = 7)	$OPN^{-/-}$ (n = 4)
BrdUrd	Papilloma	++*	++	+++	+++
	Epidermis	3.68 ± 1.86 †	3.13 ± 0.67	2.95 ± 1.25	2.75 ± 2.14
TUNEL	Papilloma	9.06 ± 7.89 ‡	28.13 ± 6.71	9.81 ± 8.62	14.62 ± 5.12
	Epidermis	0 ± 0§	0.20 ± 0.20	0 ± 0	0.25 ± 0.25

*Quantitation of BrdUrd staining in papillomas. The total number of BrdUrd-stained cells from five randomly selected fields at ×40 magnification per papilloma or sample was obtained. The number obtained was then averaged by the number of mice (n) to obtain the number of BrdUrd signals per sample, which was then scored as follows: +, <20 cells; ++, between 20 and 50 cells; +++, >50 cells per sample.

†Quantitation of BrdUrd staining in the epidermis surrounding papillomas. The average number of BrdUrd-positive cells from 10 fields at ×10 magnification per epidermis section or sample was obtained. The number obtained was then averaged by the number of mice (n) to obtain the number of positive signals ± SD per sample.

‡Quantitation of TUNEL-positive cells in papillomas. The total number of positive signals from five randomly selected fields at ×40 magnification per papilloma of similar morphology [i.e., finger, such as projections (see Fig. 4)] was obtained. The number obtained was then averaged by the number of mice (n) ± SD as indicated above.

§Quantitation of TUNEL-positive cells in the epidermis. The average number of TUNEL-positive cells from 10 fields per epidermis section or sample was assessed. The number obtained was then averaged by the number of mice (n) ± SD as indicated above.

stimulates cell proliferation and/or prevents cell apoptosis and thereby facilitates tumorigenesis. In addressing these possibilities, we focused our studies on the early stages of tumor development *in vivo*. Tumor promoter-induced osteopontin expression does not seem to mediate TPA-induced epidermal hyperplasia/cell proliferation because osteopontin-null skin treated thrice with TPA or for 11 weeks in a DMBA/TPA protocol showed a similar increase in epidermal thickness as WT skin. Likewise, BrdUrd labeling of osteopontin-null and WT papillomas and their adjacent epidermis show no differences in proliferative capacity.

Osteopontin expression in WT papillomas was localized in the upper spinous and granular layers. There seemed to be a greater number of apoptotic cells in these layers in osteopontin-null papillomas than in WT mice; however, quantification analyses did not show a significant difference. The lack of statistical differences in the number of apoptotic cells could be due to the wide variety of papilloma morphology, rendering it difficult to assess the significance of this finding, or that these papillomas are entering the progression stage where additional mutations and epigenetic changes are occurring. To more specifically address whether osteopontin prevents cellular apoptosis, assays for DMBA-induced apoptosis were done on the epidermis of osteopontin-null and WT mice. We found that osteopontin-null mice have significantly more apoptotic cells in the basal layer of dorsal epidermis when compared with WT mice. Because papillomas are thought to be derived from the basal cell layer and/or the squamous cell layer (34), we postulated that induced osteopontin synthesis and secretion could enhance the survival of both normal and carcinogen-initiated epidermal cells.

Papillomas derived from initiation by DMBA commonly show mutation in codon 61 of *Ha-ras* gene and also high levels of its transcript (35). Because the promoter of *spp1* gene (osteopontin) contains a ras-activated enhancer shown to mediate ras-activated expression of osteopontin (30), it is likely that the observed osteopontin expression in the DMBA/TPA-treated epidermis is regulated partly through the ras activation. In this scenario, constitutively activated ras in DMBA-initiated cells would stimulate synthesis and secretion of osteopontin, which in turn, by an autocrine route, would inhibit apoptosis of these mutated cells. Moreover, the repetitive application of the tumor promoter TPA maintains a persistent presence of osteopontin and possibly reinforces long-term survival of these initiated cells in the tumor promotion stage.

Studies by others using *in vitro* and *in vivo* models suggest that osteopontin may prevent apoptosis through integrins and/or CD44s or its variant forms. Osteopontin has been shown to enhance cell survival of interleukin-3-dependent pro-B cells and multiple myeloma cells by engaging with CD44 (9) and CD44v 6, respectively (36). The prosurvival effect of osteopontin ligating to CD44 was shown to be mediated through activation of PI3K and Akt (9). Interestingly, murine epidermis has been reported to express CD44s and the variant forms, such as CD44v 6 and CD44v 10 (37, 38).

Besides mediating an antiapoptosis effect through CD44s and its variants, integrin-mediated adhesion of cells to osteopontin has also been shown to induce a prosurvival effect. Adhesion of osteopontin to $\alpha_v\beta_3$ enhances the survival of melanocytes (39) and endothelial cells presumably through the nuclear factor-κB pathway (40, 41). Interestingly, though, murine and human keratinocytes normally do not express the β_3 integrin subunit (42, 43). This is consistent with our findings of murine epidermal-like JB6 cells (29). These cells also express CD44s but do not mediate attachment to osteopontin. Instead, TPA activates the integrin receptor (possibly $\alpha_v\beta_5$) to increase its affinity or avidity to the RGD cell-binding region of osteopontin (29). Whether or not TPA activates or up-regulates integrin and/or CD44s expression and which receptors interact with osteopontin in murine epidermis remains to be investigated.

Nevertheless, the ligation of matrix proteins to integrin receptors has been shown to activate focal adhesion kinases (FAK). Furthermore, papilloma formation is suppressed in FAK-null mice in two-stage skin chemical carcinogenesis studies (44). These findings further support the importance of matricellular protein interaction with integrins in regulating tumor development.

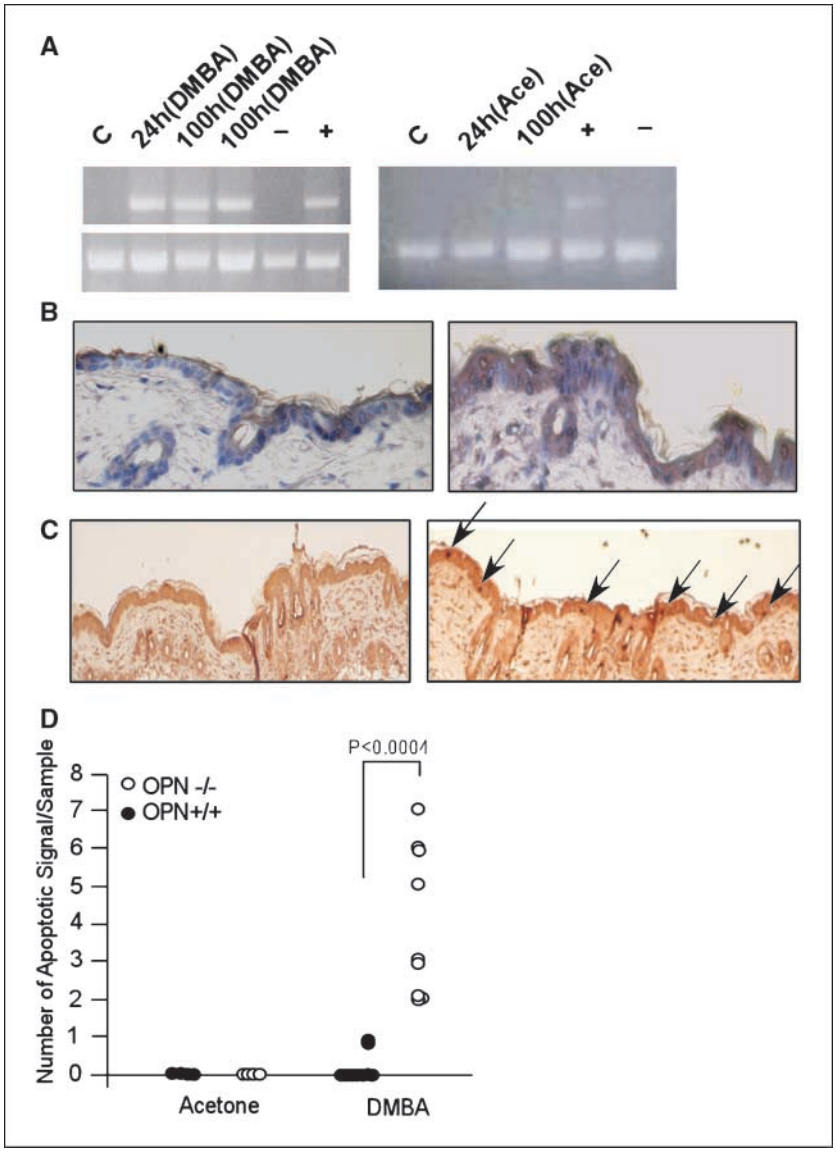

Figure 5. DMBA-induced apoptosis in the epidermis of osteopontin-null and WT mice. *A,* semiquantitative RT-PCR of osteopontin expression in mouse skin from WT and osteopontin-null mice treated with DMBA or acetone. Dorsal skin was treated once with 20 μmol/L DMBA or 200 μL acetone. Skin samples were harvested at 24 and 100 hours after DMBA treatment, total RNA was extracted, and semiquantitative RT-PCR was done to quantify osteopontin expression. *Left* and *right, lane C,* WT mouse skin without treatment; *lanes* + and −, TPA- or DMSO-treated mouse epidermal, such as JB6 Cl41.5a cells, respectively. *B,* immunohistochemical analyses of osteopontin expression in the epidermis. WT skin treated with acetone (*left*) or DMBA (*right*) was harvested at 100 hours after treatment. Tissue sections were treated with 5 μg/mL rabbit IgG (data not shown) or antibody to rat osteopontin. *C,* TUNEL analyses of apoptotic cells in WT and osteopontin-null mice treated with DMBA. *Left,* WT skin; *right,* osteopontin-null skin. WT and osteopontin-null mice were treated with DMBA (5 mice per group) or acetone (4 mice per group), and skin sections were obtained from the upper dorsal region of each mouse. Tissue sections from the upper dorsal region were analyzed for apoptotic cells. *Arrows,* apoptotic cells. *D,* graph of the number of TUNEL-positive cells in the basal cell layer of WT and osteopontin-null mice treated with DMBA. Upper dorsal mouse skin was treated with DMBA as described in (*C*). For DMBA-treated WT or osteopontin-null skin ($n = 10$) with two samples per mouse from five mice. For acetone-treated WT or osteopontin-null skin ($n = 4$) with one sample per mouse from four mice. Data analyses were done using paired *t* test.

Although this study supports the role of osteopontin in enhancing cell survival, this may not be the only mechanism by which osteopontin acts to drive tumor promotion. It is also possible that osteopontin enhances angiogenesis *in vivo*. However, identification of an appropriate animal model to be used without TPA (a confounding factor in carcinogenesis studies) will be necessary to address this mechanism. Another important observation is the specificity of osteopontin deletion in restricting tumorigenesis but not cell proliferation or hyperplasia. This phenomenon has been observed in three other studies. First, in the transgenic mice expressing activator protein-1 inhibitor TAM67, tumor promotion was inhibited but hyperplasia was unaffected (45). Second, mice lacking protein kinase Cα show impaired TPA-induced epidermal hyperplasia with enhanced tumor formation (46). Third, keratin 10-null mice show increase cell proliferation but decrease tumor development in skin chemical carcinogenesis experiment (47). These studies suggest that epidermal hyperplasia is not always necessary to drive tumor promotion.

In conclusion, this is the first *in vivo* study using the two-stage skin chemical carcinogenesis protocol to directly address the role of the matricellular protein osteopontin in tumor promotion. The lack of osteopontin expression markedly suppressed papilloma development. Experimental evidence suggests that promoter-induced osteopontin expression plays a critical role in regulating the rate-limiting step of tumor promotion, possibly by providing the initiated cells a conducive environment in which to prolong their survival and, consequently, facilitate tumor development.

Acknowledgments

Received 3/16/2006; revised 5/4/2006; accepted 5/10/2006.

Grant support: NIH grants R01 CA90920 (P-L. Chang) and P30-AR, Veterans Affairs grant (C. Elmets), and University of Alabama at Birmingham Comprehensive Cancer Center. The development and maintenance of the original osteopontin-null line was supported by NIH grant P20RR1555 (R. Friesel and L. Liaw) from the National Center for Research Resources.

The costs of publication of this article were defrayed in part by the payment of page charges. This article must therefore be hereby marked *advertisement* in accordance with 18 U.S.C. Section 1734 solely to indicate this fact.

We thank Jane Hosmer, Camille Effler, and Louie Harkins for doing paraffin embedding, cutting sections, and staining the tissues with H&E; Dr. Casey Weaver for housing and breeding our mice in his Mouse Breeding Core facility and the Animal Resource Program for maintenance; and Chu-Yan Song and Dr. Susan Sell for the speed congenic analyses.

References

1. Weaver VM, Fischer AH, Peterson OW, et al. The importance of the microenvironment in breast cancer progression: recapitulation of mammary tumorigenesis using a unique human mammary epithelial cell model and a three-dimensional culture assay. Biochem Cell Biol 1996;74:833–51.
2. Sanders RJ, Mainiero F, Giancotti FG. The role of integrins in tumorigenesis and metastasis. Cancer Invest 1998;16:329–44.
3. Denhardt DT, Noda M. Osteopontin expression and function: role in bone remodeling. J Cell Biochem Suppl 1998;30:92–102.
4. Rittling SR, Denhardt DT. Osteopontin function in pathology: lessons from osteopontin-deficient mice. Exp Nephrol 1999;7:103–13.
5. Chang PL, Prince CW. 1α,25-Dihydroxyvitamin D3 stimulates synthesis and secretion of nonphosphorylated osteopontin (secreted phosphoprotein 1) in mouse JB6 epidermal cells. Cancer Res 1991;51:2144–50.
6. Christensen B, Nielsen MS, Haselmann KF, et al. Posttranslationally modified residues of native human osteopontin are located in clusters. Identification of thirty-six phosphorylation and five *O*-glycosylation sites and their biological implications. Biochem J 2005;390:285–92.
7. Yokosaki Y, Matsuura N, Sasaki T, et al. The integrin α(9)β(1) binds to a novel recognition sequence (SVVYGLR) in the thrombin-cleaved amino-terminal fragment of osteopontin. J Biol Chem 1999;274:36328–34.
8. Zheng DQ, Woodard AS, Tallini G, et al. Substrate specificity of α(v)β(3) integrin-mediated cell migration and phosphatidylinositol 3-kinase/AKT pathway activation. J Biol Chem 2000;275:24565–74.
9. Lin YH, Yang-Yen HF. The osteopontin-CD44 survival signal involves activation of the phosphatidylinositol 3-kinase/Akt signaling pathway. J Biol Chem 2001;276:46024–30.
10. Rittling SR, Chambers AF. Role of osteopontin in tumour progression. Br J Cancer 2004;90:1877–81.
11. Rittling SR, Matsumoto HN, McKee MD, et al. Mice lacking osteopontin show normal development and bone structure but display altered osteoclast formation *in vitro*. J Bone Miner Res 1998;13:1101–11.
12. Liaw L, Birk DE, Ballas CB, et al. Altered wound healing in mice lacking a functional osteopontin gene (spp1). J Clin Invest 1998;101:1468–78.
13. Tiniakos DG, Yu H, Liapis H. Osteopontin expression in ovarian carcinomas and tumors of low malignant potential (LMP). Hum Pathol 1998;29:1250–4.
14. Kusafuka K, Yamaguchi A, Kayano T, et al. Expression of bone matrix proteins, osteonectin and osteopontin, in salivary pleomorphic adenomas. Pathol Res Pract 1999;195:733–9.
15. Devoll RE, Li W, Woods KV, et al. Osteopontin (OPN) distribution in premalignant and malignant lesions of oral epithelium and expression in cell lines derived from squamous cell carcinoma of the oral cavity. J Oral Pathol Med 1999;28:97–101.
16. Thalmann GN, Sikes RA, Devoll RE, et al. Osteopontin: possible role in prostate cancer progression. Clin Cancer Res 1999;5:2271–7.
17. Koopmann J, Fedarko NS, Jain A, et al. Evaluation of osteopontin as biomarker for pancreatic adenocarcinoma. Cancer Epidemiol Biomarkers Prev 2004;13:487–91.
18. Chang PL, Cao M, Hicks P. Osteopontin induction is required for tumor promoter-induced transformation of preneoplastic mouse cells. Carcinogenesis 2003;24:1749–58.
19. Hashimoto Y, Tajima O, Hashiba H, et al. Elevated expression of secondary, but not early, responding genes to phorbol ester tumor promoters in papillomas and carcinomas of mouse skin. Mol Carcinog 1990;3:302–8.
20. Craig AM, Denhardt DT. The murine gene encoding secreted phosphoprotein 1 (osteopontin): promoter structure, activity, and induction *in vivo* by estrogen and progesterone. Gene 1991;100:163–71.
21. Craig AM, Smith JH, Denhardt DT. Osteopontin, a transformation-associated cell adhesion phosphoprotein, is induced by 12-*O*-tetradecanoylphorbol 13-acetate in mouse epidermis. J Biol Chem 1989;264:9682–9.
22. Craig AM, Bowden GT, Chambers AF, et al. Secreted phosphoprotein mRNA is induced during multi-stage carcinogenesis in mouse skin and correlates with the metastatic potential of murine fibroblasts. Int J Cancer 1990;46:133–7.
23. Lasa M, Chang PL, Prince CW, et al. Phosphorylation of osteopontin by Golgi apparatus casein kinase. Biochem Biophys Res Commun 1997;240:602–5.
24. Unni E, Kittrell FS, Singh U, et al. Osteopontin is a potential target gene in mouse mammary cancer chemoprevention by Se-methylselenocysteine. Breast Cancer Res 2004;6:586–92.
25. Fan Q, Ding J, Zhang J, et al. Effect of the knockdown of podocin mRNA on nephrin and α-actinin in mouse podocyte. Exp Biol Med 2004;229:964–70.
26. Sisskin EE, Gray T, Barrett JC. Correlation between sensitivity to tumor promotion and sustained epidermal hyperplasia of mice and rats treated with 12-*O*-tetra-decanoylphorbol-13-acetate. Carcinogenesis 1982;3:403–7.
27. Smith JH, Denhardt DT. Molecular cloning of a tumor promoter-inducible mRNA found in JB6 mouse epidermal cells: induction is stable at high, but not at low, cell densities. J Cell Biochem 1987;34:13–22.
28. Chang PL, Tucker MA, Hicks PH, et al. Novel protein kinase C isoforms and mitogen-activated kinase kinase mediate phorbol ester-induced osteopontin expression. Int J Biochem Cell Biol 2002;34:1142–51.
29. Chang PL, Chambers AF. Transforming JB6 cells exhibit enhanced integrin-mediated adhesion to osteopontin. J Cell Biochem 2000;78:8–23.
30. Guo X, Zhang YP, Mitchell DA, et al. Identification of a ras-activated enhancer in the mouse osteopontin promoter and its interaction with a putative ETS-related transcription factor whose activity correlates with the metastatic potential of the cell. Mol Cell Biol 1995;15:476–87.
31. Wai PY, Kuo PC. The role of osteopontin in tumor metastasis. J Surg Res 2004;121:228–41.
32. Feng F, Rittling SR. Mammary tumor development in MMTV-c-myc/MMTV-v-Ha-ras transgenic mice is unaffected by osteopontin deficiency. Breast Cancer Res Treat 2000;63:71–9.
33. Crawford HC, Matrisian LM, Liaw L. Distinct roles of osteopontin in host defense activity and tumor survival during squamous cell carcinoma progression *in vivo*. Cancer Res 1998;58:5206–15.
34. Morris RJ, Coulter K, Tryson K, et al. Evidence that cutaneous carcinogen-initiated epithelial cells from mice are quiescent rather than actively cycling. Cancer Res 1997;57:3436–43.
35. Pelling JC, Fischer SM, Neades R, et al. Elevated expression and point mutation of the Ha-ras proto-oncogene in mouse skin tumors promoted by benzoyl peroxide and other promoting agents. Carcinogenesis 1987;8:1481–4.
36. Caers J, Gunthert U, De Raeve H, et al. The involvement of osteopontin and its receptors in multiple myeloma cell survival, migration, and invasion in the murine 5T33MM model. Br J Haematol 2005;132:469–77.
37. Liu K, Kasper M, Bierhaus A, et al. Differential expression of CD44s and CD44v10 proteins and syndecan in normal and irradiated mouse epidermis. Histochem Cell Biol 1997;107:159–67.
38. Milstone LM, Hough-Monroe L, Kugelman LC, et al. Epican, a heparan/chondroitin sulfate proteoglycan form of CD44, mediates cell-cell adhesion. J Cell Sci 1994;107:3183–90.
39. Geissinger E, Weisser C, Fischer P, et al. Autocrine stimulation by osteopontin contributes to antiapoptotic signalling of melanocytes in dermal collagen. Cancer Res 2002;62:4820–8.
40. Scatena M, Almeida M, Chaisson ML, et al. NF-κB mediates $\alpha_v\beta_3$ integrin-induced endothelial cell survival. J Cell Biol 1998;141:1083–93.
41. Khan SA, Lopez-Chua CA, Zhang J, et al. Soluble osteopontin inhibits apoptosis of adherent endothelial cells deprived of growth factors. J Cell Biochem 2002;85:728–36.
42. Carroll JM, Romero MR, Watt FM. Suprabasal integrin expression in the epidermis of transgenic mice results in developmental defects and a phenotype resembling psoriasis. Cell 1995;83:957–68.
43. Kubo M, Van de Water L, Plantefaber LC, et al. Fibrinogen and fibrin are anti-adhesive for keratinocytes: a mechanism for fibrin eschar slough during wound repair. J Invest Dermatol 2001;117:1369–81.
44. McLean GW, Komiyama NH, Serrels B, et al. Specific deletion of focal adhesion kinase suppresses tumor formation and blocks malignant progression. Genes Dev 2004;18:2998–3003.
45. Young MR, Li JJ, Rincon M, et al. Transgenic mice demonstrate AP-1 (activator protein-1) transactivation is required for tumor promotion. Proc Natl Acad Sci U S A 1999;96:9827–32.
46. Hara T, Saito Y, Hirai T, et al. Deficiency of protein kinase Cα in mice results in impairment of epidermal hyperplasia and enhancement of tumor formation in two-stage skin carcinogenesis. Cancer Res 2005;65:7356–62.
47. Reichelt J, Furstenberger G, Magin TM. Loss of keratin 10 leads to mitogen-activated protein kinase (MAPK) activation, increased keratinocyte turnover, and decreased tumor formation in mice. J Invest Dermatol 2004;123:973–81.